

Predicting Fundamental Gaps of Chromium-Based 2D Materials Using GW Methods

Miroslav Kolos and František Karlický*

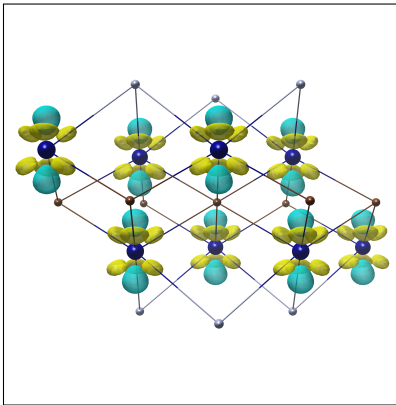
Department of Physics, Faculty of Science, University of Ostrava, 30. dubna 22, 701 03 Ostrava, Czech Republic

E-mail: frantisek.karlicky@osu.cz

Abstract

Precise and accurate predictions of the two-dimensional (2D) material's fundamental gap are crucial for next-generation flexible electronic and photonic devices. We, therefore, evaluated the predictivity of the GW approach in its several variants built on various density functional theory (DFT) inputs. We identified reasons for significant discrepancies between generalized gradient approximation and hybrid DFT results for intricate cases of 2D materials containing chromium and evaluated the diverse behavior of subsequent quasiparticle corrections. We examined the impact of omitted vertex corrections using the more computationally intensive quasiparticle self-consistent QPGW and partially self-consistent QPGW₀ methodologies. We observed consistent trends across Cr-based and other 2D materials compared by advanced GW calculations, suggesting that single-shot G₀W₀@PBE can provide reasonable estimates of fundamental gaps when applied with caution. While this approach shows promise for a variety of 2D materials, including complicated antiferromagnetic chromium-based transition metal carbides (MXenes), further research is required to validate its reliability for strongly correlated systems. In contrast, the G₀W₀@HSE06 approach may strongly overestimate gaps in some cases.

TOC Graphic



1. INTRODUCTION

The fundamental gap is an important property of any new material. Namely, gaps in semiconducting and insulating materials have been of critical importance for applications and industry for a long time,¹ and reliable predictions of fundamental gaps are therefore needed. Density functional theory (DFT) approximates the fundamental gap (defined using ionization energy and electron affinity) by the electronic gap from Kohn-Sham eigenvalues.² As local and semilocal DFT strongly underestimate the band gaps of semiconduc-

tors and insulators due to self-interaction error,³ the band gap problem is solved by many-body methods or often effectively overcome by hybrid density functionals.² The same is valid in recent research on a new generation of atomically thin films of semiconducting and insulating materials, two-dimensional (2D) materials, with the unique potential to fabricate flexible and ultrathin devices.⁴ Despite that DFT and many-body methods behave quite standardly in 2D materials, in our recent investigations,⁵ we discovered a chromium puzzle when we explored the electronic properties of transition metal car-

bides (MXenes), specifically Cr_2CF_2 and $\text{Cr}_2\text{C}(\text{OH})_2$. First of all, the hybrid HSE06 density functional⁶ surprisingly provided an electronic band gap value of more than 300% of the one from generalized gradient approximation (GGA) of DFT by Perdew-Burke-Erzenhof (PBE).⁷ Such a significant difference is not typically observed.^{8,9} This discrepancy highlights potential limitations in conventional computational methods for studying transition-metal-based systems like those considered here. Further, our careful studies (see below) on complicated semiconducting antiferromagnetic (AFM) Cr_2CF_2 MXene using many-body GW approximation¹⁰ in time-proven single-shot G_0W_0 @PBE version revealed a band gap that is unexpectedly lower than that from hybrid HSE06 calculations. Given that GW methods are approximations of Hedin’s exact equations¹⁰ and depend on the input wavefunction quality, we conducted further studies to investigate these disparities between PBE and HSE06 density functionals to clarify the unusual behavior observed in MXenes and check general properties of hybrid functionals and GW methods for 2D materials. Converged fundamental gaps from G_0W_0 @PBE are considered as a reference, and band gaps obtained from HSE06 on the other hand are considered as a practical compromise. We aim to test whether these considerations are valid for such complicated materials.

2. COMPUTATIONAL DETAILS

Our study utilizes the Vienna ab initio simulation package (VASP) with the projector augmented wave (PAW) method for comprehensive electronic structure calculations.^{11,12} We employ GW-specific PAWs, treating s and p electrons explicitly, with d electrons included for chromium and scandium. Atomic positions are optimized using density functional theory (DFT) with the Perdew-Burke-Ernzerhof (PBE) functional,⁷ applying the conjugate gradient algorithm until forces are below 10^{-3} eV/Å. Electronic steps achieve self-consistent field (SCF) convergence at 10^{-7} eV, with a plane-wave basis set energy cut-off of 400 eV. Lattice vibrational frequencies for Cr_2CF_2 are calculated using PBE within Phonopy,¹³ with a 0.01 Å displacement and an $8\times 8\times 1$ supercell (section S1 in SI). To enhance electronic structure accuracy, we incorporate the HSE06 hybrid functional,⁶ which combines Hartree-Fock exact exchange with PBE exchange-correlation. We used the G_0W_0 approximation, involving Green’s function G , and screened Coulomb potential W with input orbitals from PBE density functional (see section S2 in SI for settings and convergences) and HSE06 density functional. Our approach also includes full self-consistent quasiparticle QPGW and QPGW₀ calculations, updating wavefunctions at each iteration.¹⁴ G in QPGW₀ and both G and W in QPGW are recalculated using updated quasiparticle energies and refined wavefunctions (section S3 in SI). Quasiparticle gaps were subtracted from conduction band minimum (CBM) and valence band maximum (VBM) energies.

3. RESULTS AND DISCUSSION

Before investigating the discrepancies between PBE and HSE06 observed in Cr_2CF_2 , we first studied its stability and preferred structural conformer. Our analysis found that the preferred and stable structure is trigonal (particularly trigonal type 2; for details, see the Supporting Informa-

tion (SI)). To gain a deeper understanding of the discrepancies between PBE and HSE06, we expanded our investigation and based our considerations on three 2D materials: two simpler (s,p -containing elements), hexagonal boron nitride (BN) and fluorographene (CF), and one more difficult scandium-based MXene $\text{Sc}_2\text{C}(\text{OH})_2$. These 2D materials were selected because their carefully converged electronic G_0W_0 @PBE band gaps are in perfect agreement with experiment (layered bulk BN)¹⁵ and quantum Monte Carlo (QMC) (CF and $\text{Sc}_2\text{C}(\text{OH})_2$).^{16,17} These materials’ precise and accurate G_0W_0 @PBE fundamental gaps are presented in Table 1. We performed the same procedure of careful convergence of technical parameters in G_0W_0 @PBE for Cr_2CF_2 (see SI for details), and after considerations introduced later in this paper, we added band gap to this set too. This selection of 2D materials aims to confirm the predictive accuracy of G_0W_0 @PBE for complicated chromium-based MXenes, enhancing our understanding of the electronic properties of diverse 2D materials.

Table 1: Precise G_0W_0 @PBE direct (indirect) band gap values of four 2D materials in eV.

Material	G_0W_0 Gap	Experiment/QMC	Reference
BN ^a	6.53 (6.08)	6.42 ¹⁸ (6.08 ± 0.015 ¹⁹)	Kolos <i>et al.</i> ¹⁵
CF	7.14	7.1 ± 0.1	Dubecký <i>et al.</i> ¹⁶
$\text{Sc}_2\text{C}(\text{OH})_2$	1.28	1.30 ± 0.2	Dubecký <i>et al.</i> ¹⁷
Cr_2CF_2	2.41 (2.29) ×	×	This work

^a AA’ stacking of layered BN; precise G_0W_0 @PBE band gap for monolayer BN is 7.64 (6.94) from Kolos *et al.*²⁰

Our primary focus starts with understanding the essence of the vast differences between band gaps obtained from GGA PBE and hybrid HSE06 density functionals in chromium MXenes (e.g., Cr_2CF_2 indirect gap of 1.11 eV vs. 3.27 eV, respectively) because subsequent quasiparticle corrections are dependent on input DFT wave functions and eigenvalues. The discrepancies between one-electron methods can be associated with chromium’s half-filled 3d orbitals, which exhibit a complex electronic landscape with complicated electron-electron interactions. Standard DFT methods use exchange-correlation functionals such as PBE to describe complicated electron-electron interactions. PBE, thanks to a good approximation of electronic screening, is believed to give reasonable values of macroscopic dielectric constant.²¹ On the other hand, HSE06 is a range-separated hybrid functional combining a short-range component of 25% Hartree-Fock exact exchange with 75% PBE exchange while retaining the full PBE correlation. The differences in macroscopic dielectric constant from PBE and HSE06 are vast in chromium MXene, up to nearly three times, compared to other studied 2D materials, where there are just minor changes (Tab. 2). This first hint urges a deeper study of PBE and HSE06 results for these chromium-based 2D materials.

We looked at charge density itself to understand what caused such differences between two density functionals. A striking observation was the substantial differences in electron density between the PBE and HSE06 functionals, as depicted in Figure 1. No such differences were observed in other

Table 2: Macroscopic dielectric constants for various 2D materials in various theory levels.^a

	BN	CF	Sc ₂ C(OH) ₂	Cr ₂ CF ₂ ^{AFM}	Cr ₂ CF ₂ ^{NM}
PBE	1.51	1.68	4.85	7.68	16.24
HSE06	1.38	1.56	3.14	3.18	5.69
QPGW ₀ @PBE	1.52	1.69	4.49	5.58	18.61
QPGW ₀ @HSE06	1.40	1.56	3.02	2.84	6.11
QPGW	1.33	1.46	2.68	2.83	8.70

^a All presented 2D materials are calculated using cell size of $\approx 20\text{\AA}$ in the z-direction because, in the ∞ limit, these values are always 1.²² This table, therefore, serves to compare different approaches.

studied 2D materials in our set (BN, CF, and Sc₂C(OH)₂) on the same isosurface level. To determine whether these discrepancies could be attributed to variations in magnetic moments – a known difference between PBE and HSE06²³ – we examined both magnetic and nonmagnetic (NM) (open-shell and closed-shell) forms of Cr₂CF₂. Remarkably, even in nonmagnetic configurations, notable differences in charge densities persisted (Fig. 1), indicating that these variations are intrinsic to the chromium atoms rather than influenced by magnetic properties. This is also supported by significant differences in Hartree energy between PBE and HSE06 (Tab. S2).

In order to assess whether the termination groups could influence these discrepancies, we analyzed Cr₂C(OH)₂, another antiferromagnetic material (Fig. 1). The results clearly demonstrated that the observed differences in electron density are explicitly associated with the chromium atoms, confirming that the termination groups do not contribute to the observed discrepancies. Expanding the scope of our investigation into the charge density HSE06/PBE differences, we included MXenes containing titanium and manganese elements, each exhibiting distinct magnetic properties. In all cases, no differences in charge density between PBE and HSE06 were observed at the same isosurface levels, reinforcing chromium’s unique challenge in accurately modeling electron density. We did an integration of its absolute values to quantify the differences in charge densities. We used a threshold value for differences included in the integration, consistent for all materials to include just these high-order differences and exclude vacuum noise. These results are presented in Table S3, and it is visible that MXenes containing chromium have about one order of magnitude higher differences than other materials. Similar behavior of charge density differences between PBE and HSE06, but less pronounced, was also observed in simpler 2D materials containing chromium from families of transition metal dichalcogenides and oxides (CrS₂, CrHS₂, and CrO₂; Fig. S3). It is visible that these less correlated chromium 2D materials show more minor absolute differences in Bader charge analysis (Tab. S3). Such an unexpected behavior of charge density suggests evaluating electron-electron interactions in chromium MXenes on a higher level of theory.

To address the inconsistencies in electron-electron interaction modeling in chromium-based 2D materials compared to other 2D materials, we adopted the many-body GW method,

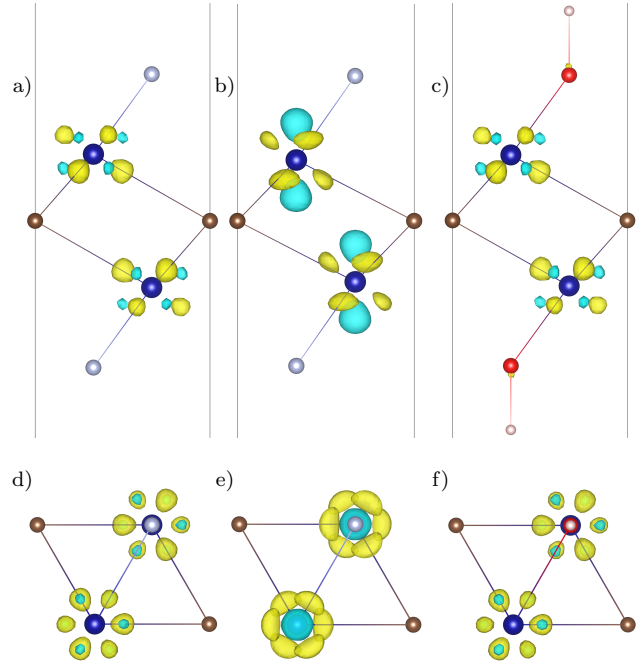


Figure 1: Differences in charge densities from PBE and HSE06 density functionals ($n_{\text{PBE}} - n_{\text{HSE06}}$) at the same isosurface level ($3.5 \cdot 10^{-5}e$) as side and top views of a),d) Cr₂CF₂^{AFM}, b),e) Cr₂CF₂^{NM}, and d),f) Cr₂C(OH)₂^{AFM}, all with highlighted unit cell boundaries in a)-c). Atom colors: brown-C, blue-Cr, grey-F, red-O, white-H. All other studied 2D materials have no visible differences at the same isosurface level.

which more accurately accounts for these interactions, yet without including vertex corrections.¹⁴ Specifically, we explored various levels of GW, including the standard single-shot corrections G₀W₀, and the more sophisticated quasiparticle self-consistent QPGW and partially self-consistent QPGW₀ methods. Notably, all these iterative QPGW approximations omit vertex corrections as specified in Hedin’s equations, which leads to the systematic overestimation of band gaps due to the absence of part of the electron-electron interactions in the self-consistent versions.¹⁴

Our findings are summarized in Figure 2, showing the relative differences in calculated fundamental gaps from the baseline G₀W₀@PBE (values from Tab. 1), with further methodological discussion available in the Supplementary Information. One striking result is the significant discrepancy between the HSE06-based results for the Cr₂CF₂ band gap and all other outcomes, highlighting the limitations of using HSE06-derived input wave functions for GW calculations. This indicates a divergence in the treatment of electron-electron interactions in chromium-based MXenes.

Importantly, our findings reveal that the behavior of relative differences between QPGW₀@PBE and G₀W₀@PBE closely mirrors across all tested 2D materials, including the problematic Cr₂CF₂. QPGW₀ methods use screened Coulomb potential W₀ calculated from non-interacting Green’s function on input orbitals (PBE, HSE06). Full self-consistency is achieved by updating energies and wavefunctions based on Green’s repeated propagation through the system with PBE/HSE06-based screened coulomb interaction. This

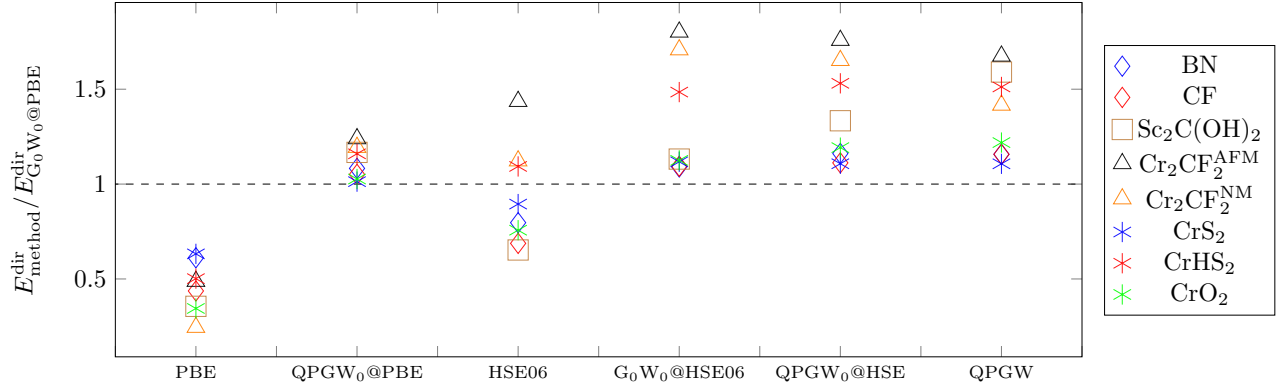


Figure 2: Fundamental gaps of several 2D materials obtained from different methods (abbreviated in x-axis labels) divided by the corresponding $G_0W_0@PBE$ fundamental gap, presented as a horizontal dashed line.

method, therefore, shows how reasonable the input orbitals were, and therefore, PBE input orbitals seem to be reasonable regardless of the system. Noting that $G_0W_0@PBE$ band gap results for BN, CF, and $Sc_2C(OH)_2$ were proven to be precise and accurate, and aforementioned similar behavior of relative differences between $G_0W_0@PBE$ and $GW_0@PBE$ for all studied materials (Cr_2CF_2 including), this could be interpreted that $G_0W_0@PBE$ provides reliable predictions currently achievable without vertex corrections, even for complicated chromium-based 2D materials. However, due to the lack of experimental or high-level quantum chemistry calculations specifically supporting the precision of $G_0W_0@PBE$ for Cr_2CF_2 , caution still should be exercised when generalizing its reliability for strongly correlated systems. Further research, including experimental validations and advanced computational studies, is necessary to confirm these findings for chromium-based 2D materials and other complex systems.

A crucial aspect of our research involves thoroughly examining the QPGW results. As illustrated in Figure 2, the fully self-consistent QPGW method tends to significantly overestimate the band gaps of strongly correlated or magnetic d -element-based 2D materials studied, underscoring the pivotal role of complicated electron-electron interactions. These effects are not accounted for due to the absence of vertex corrections in the GW framework, which appears particularly critical in such types of 2D materials, intensifying the overestimations. On the other hand, less correlated NM Cr materials, CrS_2 and CrO_2 , closely mirror sp -element-based 2D materials.

Our focus switches to analyzing band gap results obtained from $G_0W_0@HSE06$ and $QPGW_0@HSE06$. The results from these calculations, including QPGW, demonstrated surprisingly similar band gaps for both NM and AFM Cr_2CF_2 , with the self-consistent approaches yielding even smaller band gaps than one observed in the single-shot G_0W_0 . In principle, QPGW results overestimate band gaps;¹⁴ therefore, from our results, it is clear that HSE06 orbitals are unsuitable inputs for subsequent many-body G_0W_0 calculations for these materials because $G_0W_0@HSE06$ gaps are even larger than QPGW ones. This phenomenon is further explored by comparing charge densities from GW and

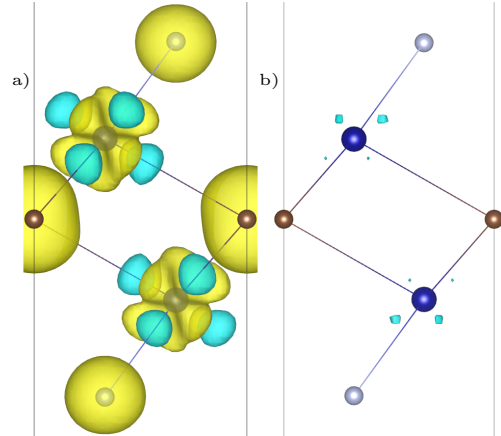


Figure 3: Differences in charge densities in Cr_2CF_2 a) $n_{QPGW_0@PBE} - n_{QPGW@PBE}$ and b) $n_{QPGW_0@HSE06} - n_{QPGW@HSE06}$, at the same isosurface level ($3.5 \cdot 10^{-6} e$).

GW_0 , using PBE and HSE06 orbitals, as detailed in Figure 3. Surprisingly, iterations of W starting from W_0 obtained from HSE06 orbitals show much smaller differences in charge density than those from PBE. This investigation led us to conclude that W_0 , derived as a single-shot screened Coulomb interaction from a non-interacting Green's function propagated through the HSE06 wave function, mimics a fully converged W . This behavior, on the one hand, proposes the credibility of HSE06, on the other hand, considering shortcoming of QPGW leading to fundamental gap overestimations (because of omitting vertex corrections),¹⁴ serves as evidence of HSE06's inadequacy as input orbitals for GW calculations for predicting the electronic structure and band gaps of such highly correlated chromium 2D materials. In addition, HSE06 overestimates magnetic moments,⁵ can fail because of multireference system²⁴ or due to tradeoffs between over-delocalization and under-binding,²⁵ and subsequent quasiparticle $G_0W_0@HSE06$ gaps often overestimate experiments in strongly correlated materials, as shown e.g. for antiferromagnetic hematite $\alpha-Fe_2O_3$.²⁶ It is important to note, however, that the $G_0W_0@HSE06$ approach is particularly valuable in the case of small-gap semiconductors, where PBE provides (artificially) negative gap and subsequent per-

turbative $G_0W_0@PBE$ is not available.¹⁴ Conversely, our findings highlight the remarkable efficiency of the PBE density functional, which consistently provides highly reliable results when used as the input for single-shot GW calculations in these challenging 2D compounds.

From our results in Figure 2, it is evident that the relative variability in GW-calculated band gaps significantly depends on the material’s electronic and magnetic properties. For nonmagnetic, weakly correlated materials such as BN, CF, CrS_2 , and CrO_2 , the maximal differences in band gaps across different levels of GW (e.g., QPGW₀, QPGW) and input orbitals do not exceed 20%. However, when considering systems with magnetic properties (e.g., $CrHS_2$) or stronger correlations (e.g., $Sc_2C(OH)_2$, $Cr_2CF_2^{NM}$), or the combination of both ($Cr_2CF_2^{AFM}$), these discrepancies increase significantly, ranging from 50 % to 80 % of the band gap. These findings highlight the need for careful consideration of GW methodologies, particularly for magnetic and strongly correlated materials, where variations in band gap predictions can be substantial.

The evaluation of the macroscopic dielectric constant across various 2D materials further underscores the reliability of the $G_0W_0@PBE$ method even for Cr_2CF_2 . As presented in Table 2, there is a substantial discrepancy between the dielectric constants calculated using PBE and HSE06 for Cr_2CF_2 , with PBE predicting a notably higher value compared to HSE06. This significant variance suggests that the choice of exchange-correlation functional profoundly impacts the predicted dielectric properties, especially in 2D materials with strong electronic interactions such as chromium-based MXenes. Interestingly, the values obtained from $G_0W_0@PBE$ are between those of PBE and HSE06, whereas $G_0W_0@HSE06$ closely aligns with the HSE06 values; note that results of the dielectric constant from G_0W_0 and GW_0 are the same, due to the same response function. This behavior provides additional validation for using $G_0W_0@PBE$ as a robust method, capturing crucial aspects of material behavior.

4. CONCLUSIONS

The most significant finding from our data is that the fundamental gap of chromium MXene Cr_2CF_2 is wider in both its magnetic and nonmagnetic forms when calculated with $G_0W_0@HSE06$ compared to the results from QPGW. Highlighting a critical limitation: fully self-consistent QPGW, in principle, overestimates band gaps due to its lack of vertex corrections, HSE06 orbitals should be used cautiously as input for G_0W_0 calculations in such highly correlated systems because such overestimation can lead to a misinterpretation of the material’s electronic properties. Additionally, our analysis revealed substantial differences in charge densities between PBE and HSE06 across all chromium-based 2D materials studied, including simpler systems such as CrS_2 , $CrHS_2$, and CrO_2 . Among these, the overestimation of the band gap by $G_0W_0@HSE06$ was observed only in magnetic $CrHS_2$. In contrast, nonmagnetic CrS_2 and CrO_2 exhibited behavior akin to sp-bonded materials, underscoring the joint impact of magnetism and correlation effects in these systems.

Interestingly, $G_0W_0@PBE$ demonstrates similar behavior

across all tested materials when contrasted with fully Green’s function self-consistent QPGW₀@PBE, where the screening is not updated. Our results allow us to conclude that with careful treatment, $G_0W_0@PBE$ remains a viable approach for achieving accurate and reliable results, even for complex materials such as chromium-based systems.

Supporting Information Available

Cr_2CF_2 conformers, phonon band structure, input DFT calculations, charge densities differences of CrS_2 , $CrHS_2$, and CrO_2 , integration of charge densities differences, the convergence of G_0W_0 calculations, and iterations evolution in full self-consistent quasiparticle QPGW calculations.

Acknowledgement This work was supported by the Czech Science Foundation (21-28709S) and the European Union under the LERCO project (number CZ.10.03.01/00/22_003/0000003) via the Operational Programme Just Transition. The computations were performed at IT4Innovations National Supercomputing Center (e-INFRA CZ, ID:90140). We thank Matúš Dubecký for helpful discussions.

REFERENCES

- (1) Capasso, F. Band-Gap Engineering: From Physics and Materials to New Semiconductor Devices. *Science* **1987**, *235*, 172–176.
- (2) Perdew, J. P.; Yang, W.; Burke, K.; Yang, Z.; Gross, E. K. U.; Scheffler, M.; Scuseria, G. E.; Henderson, T. M.; Zhang, I. Y.; Ruzsinszky, A. et al. Understanding band gaps of solids in generalized Kohn–Sham theory. *Proc. Natl. Acad. Sci. U.S.A.* **2017**, *114*, 2801–2806.
- (3) Mori-Sánchez, P.; Cohen, A. J.; Yang, W. Localization and Delocalization Errors in Density Functional Theory and Implications for Band-Gap Prediction. *Phys. Rev. Lett.* **2008**, *100*, 146401.
- (4) Chaves, A.; Azadani, J. G.; Alsalman, H.; da Costa, D. R.; Frisenda, R.; Chaves, A. J.; Song, S. H.; Kim, Y. D.; He, D.; Zhou, J. et al. Bandgap engineering of two-dimensional semiconductor materials. *npj 2D Mater. Appl.* **2020**, *4*, 29.
- (5) Ketolainen, T.; Karlický, F. Optical gaps and excitons in semiconducting transition metal carbides (MXenes). *J. Mater. Chem. C* **2022**, *10*, 3919–3928.
- (6) Heyd, J.; Scuseria, G. E.; Ernzerhof, M. Hybrid functionals based on a screened Coulomb potential. *J. Chem. Phys.* **2003**, *118*, 8207–8215.
- (7) Perdew, J. P.; Burke, K.; Ernzerhof, M. Generalized Gradient Approximation Made Simple. *Phys. Rev. Lett.* **1996**, *77*, 3865–3868.
- (8) Civalleri, B.; Presti, D.; Dovesi, R.; Savin, A. *Chemical Modelling: Applications and Theory*; The Royal Society of Chemistry, 2012.

- (9) Garza, A. J.; Scuseria, G. E. Predicting Band Gaps with Hybrid Density Functionals. *J. Phys. Chem. Lett.* **2016**, *7*, 4165–4170.
- (10) Hedin, L. New Method for Calculating the One-Particle Green's Function with Application to the Electron-Gas Problem. *Phys. Rev.* **1965**, *139*, A796–A823.
- (11) Kresse, G.; Joubert, D. From ultrasoft pseudopotentials to the projector augmented-wave method. *Phys. Rev. B* **1999**, *59*, 1758–1775.
- (12) Blöchl, P. Projector augmented-wave method. *Phys. Rev. B* **1994**, *50*, 17953–17979.
- (13) Togo, A.; Tanaka, I. First principles phonon calculations in materials science. *Scr. Mater.* **2015**, *108*, 1–5.
- (14) Grumet, M.; Liu, P.; Kaltak, M.; Klimeš, J.; Kresse, G. Beyond the quasiparticle approximation: Fully self-consistent *GW* calculations. *Phys. Rev. B* **2018**, *98*, 155143.
- (15) Kolos, M.; Karlický, F. Accurate many-body calculation of electronic and optical band gap of bulk hexagonal boron nitride. *Phys. Chem. Chem. Phys.* **2019**, *21*, 3999–4005.
- (16) Dubecký, M.; Karlický, F.; Minárik, S.; Mitas, L. Fundamental gap of fluorographene by many-body GW and fixed-node diffusion Monte Carlo methods. *J. Chem. Phys.* **2020**, *153*, 184706.
- (17) Dubecký, M.; Minárik, S.; Karlický, F. Benchmarking fundamental gap of Sc₂C(OH)₂ MXene by many-body methods. *J. Chem. Phys.* **2023**, *158*, 054703.
- (18) Doan, T. C.; Li, J.; Lin, J. Y.; Jiang, H. X. Bandgap and exciton binding energies of hexagonal boron nitride probed by photocurrent excitation spectroscopy. *Appl. Phys. Lett.* **2016**, *109*, 122101.
- (19) Cassabois, G.; Valvin, P.; Gil, B. Hexagonal boron nitride is an indirect bandgap semiconductor. *Nat. Photonics* **2016**, *10*, 262–266.
- (20) Kolos, M.; Karlický, F. The electronic and optical properties of III–V binary 2D semiconductors: how to achieve high precision from accurate many-body methods. *Phys. Chem. Chem. Phys.* **2022**, *24*, 27459–27466.
- (21) Petousis, I.; Chen, W.; Hautier, G.; Graf, T.; Schladt, T. D.; Persson, K. A.; Prinz, F. B. Benchmarking density functional perturbation theory to enable high-throughput screening of materials for dielectric constant and refractive index. *Phys. Rev. B* **2016**, *93*, 115151.
- (22) Ketolainen, T.; Macháčková, N.; Karlický, F. Optical Gaps and Excitonic Properties of 2D Materials by Hybrid Time-Dependent Density Functional Theory: Evidences for Monolayers and Prospects for van der Waals Heterostructures. *J. Chem. Theory Comput.* **2020**, *16*, 5876–5883.
- (23) Meng, Y.; Liu, X.-W.; Huo, C.-F.; Guo, W.-P.; Cao, D.-B.; Peng, Q.; Dearden, A.; Gonze, X.; Yang, Y.; Wang, J. et al. When Density Functional Approximations Meet Iron Oxides. *J. Chem. Theory Comput.* **2016**, *12*, 5132–5144.
- (24) Cho, Y.; Nandy, A.; Duan, C.; Kulik, H. J. DFT-Based Multireference Diagnostics in the Solid State: Application to Metal–Organic Frameworks. *J. Chem. Theory Comput.* **2023**, *19*, 190–197.
- (25) Janesko, B. G. Replacing hybrid density functional theory: motivation and recent advances. *Chem. Soc. Rev.* **2021**, *50*, 8470–8495.
- (26) Liao, P.; Carter, E. A. Testing variations of the GW approximation on strongly correlated transition metal oxides: hematite (α -Fe₂O₃) as a benchmark. *Phys. Chem. Chem. Phys.* **2011**, *13*, 15189–15199.